coasts

Article

Rapid, Landscape-Scale Assessment of Cyclonic Impacts on Mangrove Forests Using MODIS Imagery

AHM Mainul Islam [1,2] and Timothy J. Assal [1,*]

1 Department of Geography, Kent State University, Kent, OH 44242, USA; ahmmainul-islam@uiowa.edu
2 Department of Geographical and Sustainability Sciences, University of Iowa, Iowa City, IA 52242, USA
* Correspondence: tassal@kent.edu; Tel.: +1-(33)-06722046

Abstract: Cyclones are a key disturbance in mangrove ecosystems, but it is challenging to assess post-storm impacts over large areas, along with the recovery of these systems at broad temporal scales. Given the high frequency of these events in the Sundarbans region, prompt and consistent assessment of vegetation conditions is an important research need. Several studies have assessed the impact of an extreme cyclone event in 2007 (Sidr); however, there is little agreement between the extent and severity of the disturbance footprint of the cyclone, and very few studies attempted to assess vegetation recovery. We used a MODIS (Moderate Resolution Imaging Spectroradiometer) time series (2001–2010) to calculate monthly plant productivity anomalies in Google Earth Engine. We summarized dry season anomalies to assess post-storm vegetation change and evaluate the recovery time. Approximately 2100 km^2, primarily on the east side, were impacted by Sidr. The number of damaged pixels was reduced by 55% the following dry season (2008) and 93% in the dry season of 2009, indicating a near-full recovery 26 months after the event. Our results provide an additional line of evidence to provide a rapid assessment of the post-storm vegetation damage. The simple framework used can provide a comprehensive view of the extent of the damage, including lag effects on vegetation, in just a matter of months after the event.

Keywords: MODIS time-series; mangrove ecosystem; forest disturbance; vegetation productivity

Citation: Islam, A.M.; Assal, T.J. Rapid, Landscape-Scale Assessment of Cyclonic Impacts on Mangrove Forests Using MODIS Imagery. *Coasts* **2023**, *3*, 280–293. https://doi.org/10.3390/coasts3030017

Academic Editor: Andrew Martin Fischer

Received: 22 July 2023
Revised: 5 September 2023
Accepted: 8 September 2023
Published: 15 September 2023

1. Introduction

The Sundarbans are the largest, continuous mangrove ecosystem in the world and are considered a globally unique ecosystem [1]. The area provides abundant ecosystem services such as habitat and biodiversity [2], carbon storage [3], storm damage buffering [4–9] and mitigation of coastal erosion [10]. Cyclones originating in the Bay of Bengal [11] and associated storm surges are the most influential disaster events on the southern coast of Bangladesh [12]. Thus, the proximity of the Sundarbans along the southern coast of Bangladesh provides coastal safety to millions of people in this region as it acts as a vegetative shield in the direction of storm surges to help minimize adverse impacts [9,13]. As such, cyclones are a key disturbance in this part of the world, but it is difficult to assess the post-storm impact over large areas, along with the recovery of these systems at broad temporal scales. Given the high frequency of cyclones in the Sundarbans, assessment of vegetation conditions in a prompt and consistent manner remains an important research need.

Tropical cyclones are a natural disturbance in mangrove ecosystems as these discrete events change the physical environment and in turn disrupt the organization of the system, plant communities, and populations in it [14]. Severe cyclones cause extensive vegetation damage, including fractured crowns or blowdowns, often resulting in tree mortality [15,16]. Strong winds also remove foliage and branches from smaller mangrove trees, resulting in canopy cover loss and lower photosynthetic capacity [17]. This phenomenon disrupts the typical seasonal growth phenology of surviving mangrove trees, which can extend for several seasons. Cyclone-induced disturbance can impact forest structure, biogeochemical cycles and regeneration for years after the storm event [15]. Satellite remote sensing has been used to assess post-storm forest damages [18]; however, subsequent studies on post-storm forest recovery and comparative analysis on the performances of vegetation indices are limited.

Remote sensing is the most effective tool to monitor change in forests over large areas and has been employed in a number of forest structure studies that measure the loss of photosynthetic material due to defoliation events [19], blowdowns [20], and windstorm damage [21]. Given the link between biological events and climate, vegetation phenology has been a focus of recent mangrove remote sensing research [22,23]. Mangrove phenology is an important metric to assess changes in mangrove ecosystem productivity and the subsequent response to climate-induced disaster events [24]. This metric is influenced by vegetation morphology, species composition, and microclimate variability. Phenology phases are spatially intricate and temporally dynamic in tropical forest regions and display numerous periods of growth and senescence in a single annual cycle [25]. Satellite observations provide broad coverage of mangrove ecosystems at periodic time intervals to assess phenology, whereas traditional field methods are untenable at that scale [25]. Knowledge of spatial and temporal variability from episodic disturbances is necessary to understand mangrove forest dynamics at the landscape scale and these systems are often monitored using satellite-derived vegetation indices [26–29].

Many of the post-cyclone remote sensing studies in the Sundarbans have involved object-based image analysis, where a post-classification comparison is used to measure area change in mapped classes [30–32]. For example, Mandal and Hosaka [32] used Landsat-derived classifications to assess the damage of Sidr. This approach is very effective for measuring change from a forested class to a non-forested class; however, it is not possible to measure a change in condition within the same class [33]. Alternatively, pixel-based approaches consider the reflectance of individual pixels over time, and therefore, allow for a more direct approach to monitor the severity levels of a disturbance [34]. Dutta et al. [35] used temporal means of MODIS time-series derived disturbed pixels to determine the impact of Sidr (2007), Rashmi (2008), and Aila (2009) over the Sundarbans region but did not explicitly consider post-disturbance recovery. Zhang et al. [29] used a pixel-based approach to measure the relative condition and recovery of mangrove forest in south Florida using the satellite-derived Normalized Difference Moisture Index (NDMI) and found recovery rates from two to six years post-hurricane. However, few studies have directly focused on mangrove forest recovery in the Sundarbans.

The main objective of this study is to assess the impact of cyclone Sidr on the Bangladesh portion of the Sundarbans to better understand the impact on the vegetation condition and the post-disturbance dynamics. The motivation for this study was in part driven by a review of several other highly relevant, pixel-based studies that assessed the impact of cyclone Sidr [32,35–38]. We found little agreement between the extent and severity of the cyclone, and very few attempted to assess the vegetation recovery. Therefore, we sought to contribute a new approach and in doing so, provide another line of evidence of the impact of Sidr on the vegetation in the Sundarbans. First, we determined which freely available satellite sensors provided the necessary observations for this retrospective, rapid approach. Then we applied the framework to address the following questions: (a) What was the extent and severity of the cyclone in the Sundarbans with respect to vegetation condition? (b) How long did it take the forest to return to its pre-disturbance condition?

2. Materials and Methods

2.1. Study Area

Sundarbans mangrove forest is located in southwestern Bangladesh (60%) and eastern India (40%) [12,36] (Figure 1). In this study we focus on the Bangladesh side as the path of cyclone Sidr intersected the eastern side of Sundarbans. The Bangladesh Sundarbans constitutes 44% (nearly 6300 km^2) of the forest cover in the country and contains 65 mangrove species [1]. *Heritiera fomes* is the most influential and tallest (over 15 m) plant in the Sundarbans and several other common mangrove species include *Xylocarpus mekongensis*, *Excoecaria agalocha*, *Ceriops decundra*, *Sonneratia apetala* and *Avicennia officinalis* [1]. The distribution of plants in the Sundarbans is primarily controlled by elevation and salinity [39]. The seasonal climate of the Sundarbans is characterized as pre-monsoon (March to May), monsoon (June to September), post-monsoon (October to November), and dry winter (December to February) [40]. They also noted rainfall fluctuates between 1600 mm and 2000 mm (with over 80% received during the May–September monsoon season), while temperature varies between 11 °C to 37 °C. Cyclonic storms frequently occur during May to June and October to November along the coast of Bangladesh [39].

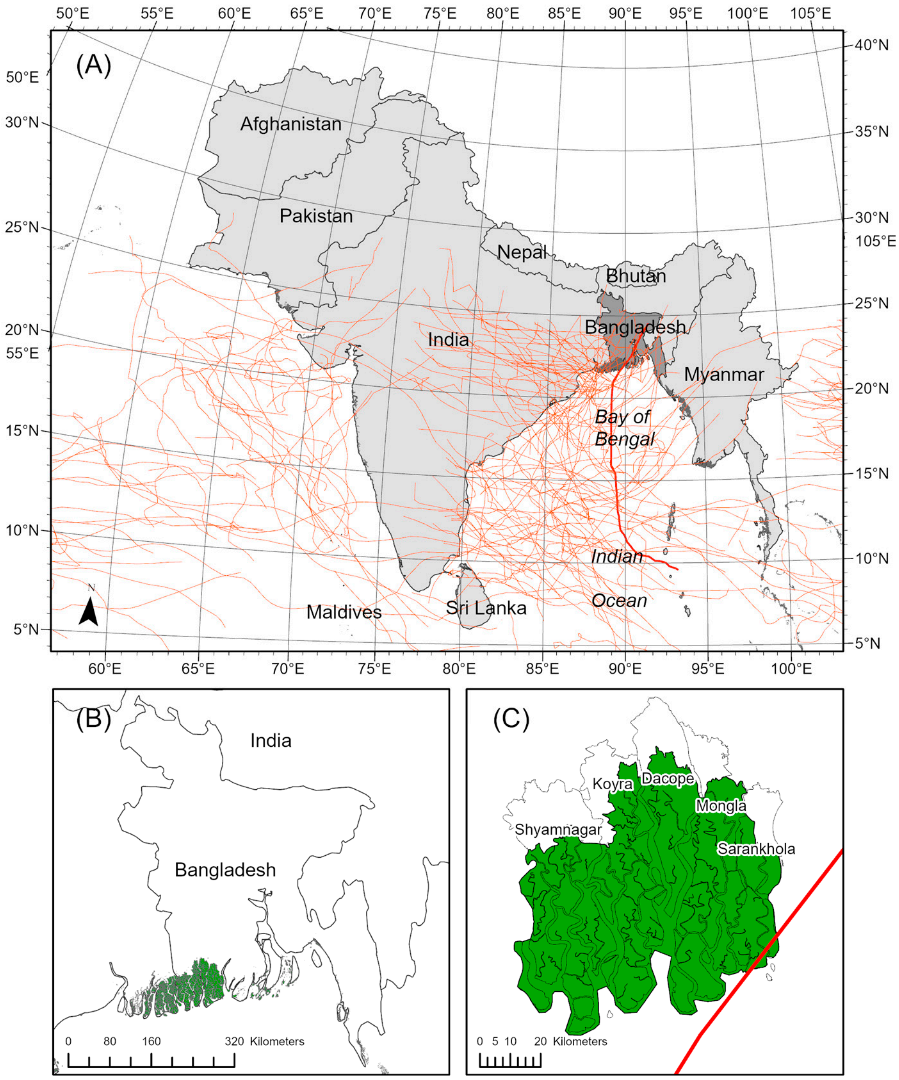

Figure 1. (**A**) Location of Bangladesh in South Asia region with cyclone tracks (2003–2023) (Sidr in red line), (**B**) Location of the Sundarbans in Bangladesh, (**C**) Upazila (a regional administration unit of Bangladesh) boundaries of the Sundarbans and Sidr trajectory in red line [41].

2.2. Cyclone Data

Cyclone data was collected from the International Best Track Archive for Climate Stewardship (IBTrACS) database [41] and the Indian Meteorological Department [42]. We followed the Saffir-Simpson hurricane wind scale to categorize the cyclones. The categories are divided into five groups: Category 1 (119–153 km h^{-1}), Category 2 (154–177 km h^{-1}), Category 3 (178–208 km h^{-1}), Category 4 (209–251 km h^{-1}), Category 5 ($\geq$252 km h^{-1}) [43]. The southern coastal region of Bangladesh is the most cyclone prone area in the country, with storms typically striking during the post-monsoon period (October–December) [42]. Sidr was a category-4 equivalent tropical cyclone that made landfall in Bangladesh on 15 November 2007, with recorded wind speeds over 213 km h^{-1} and waves of 6 m [12,36]. It was considered the second strongest cyclone since 1877 [1] and caused an estimated 10,000 deaths and $1.7 billion worth of damage [44]. The storm surge associated with Sidr overtopped the coastal area and caused massive damage to the vegetation [36]. Biotic communities of the Sundarbans were severely affected by soil erosion and winds uprooting plants, broke stems and branches of trees, and removed leaf area [1]. Of the recent cyclones that have made landfall in Bangladesh, the wind speed associated with Sidr was substantially higher (Table S1).

2.3. Satellite Data

Although Landsat data is a primary resource for remote sensing in disturbance studies, MODIS data is becoming more prominent in recent studies due to its short revisit time [45]. We utilized the MODIS Terra Surface Reflectance 8-Day Global 250 m product (MOD09Q1.006) in Google Earth Engine (GEE), a multi-petabyte open-source catalog of satellite imagery and geospatial datasets by Google. This product provides an estimate of the surface spectral reflectance and a State QA band to perform quality assurance. Surface reflectance band-1 (620–670 mm) and surface reflectance band-2 (841–876 mm) were used to calculate the Normalized Difference Vegetation Index (NDVI). We used the 8-Day composite product instead of daily reflectance because there is an additional quality assurance band available. The state QA Bitmask was used to screen the quality of pixels (bit levels 0–1 (cloud state), 2 (cloud shadow), 3–5 (land/water)).

2.4. Cloud Considerations & Minimum Observations

Collecting cloud-free images over the given study period is critical for tropical regions like Bangladesh. The southeast monsoon is the predominant feature of the Sundarbans climate, which divides the year into three distinct seasons: (i) monsoon season—June to October, (ii) cool-season—November to February, and (iii) spring season—March to June. An important consideration of the study is to collect cloud-free images in order to accurately measure vegetation productivity across a given time period. The MODIS product provided a higher temporal frequency of clear observations compared to Landsat, hence the primary rationale for using MODIS in this study. We acknowledge the tradeoff between these two sensors. Although MODIS has a lower spatial resolution compared to Landsat, the higher temporal resolution is critical for our method that has not yet been applied to this disturbance event. Monthly mean NDVI composites were generated in GEE. Clouds, cloud shadows, and water pixels were masked out from the study area before generating the monthly composites for the entire study period. A minimum observation threshold of four clear sky observations per month was enforced. This indicates the minimum number of clear sky observations needed for a given pixel to be considered in the analysis. If a pixel failed to meet the minimum valid observations within a month, it was considered insufficient data and dropped from the analysis [46]. Composites were generated for every month within the study period between 2001–2010. Monthly mean NDVI composites were exported from GEE for further processing in the R statistical software [47] using the raster package [48].

2.5. Anomaly Calculations

The selection of the optimal window of study (e.g., a month or a series of months with the highest productivity) is important for assessment of mangrove phenology and dynamics. This window is the ideal annual timeframe when the vegetation of interest is considered to be most stable. Data collected during this time is used to compare the performance of the vegetation during a given window against the long-term vegetation conditions of a reference period [49,50].

MODIS images from 2001 to 2010 were used to establish the reference period. A sum of 120 NDVI mean images were generated using GEE, where each image indicates the mean of an individual month collection. Reference periods are selected from this time series. Specific months of 2001–2007 (except November and December of 2007) were selected as reference periods because, at that time, there were no significant cyclones (last cyclone before 2001 made landfall in 2000 as per IBTrACS cyclone track) over the Bangladesh side of the Sundarbans.

NDVI anomalies were calculated for specific months between 2006 and 2010, defined as the deviation from the long-term mean of the reference period. Reference periods were selected on a monthly basis; for example, only the November months before November 2007 (November 2001, November 2002, November 2003, November 2004, November 2005, and November 2006) were used as the reference period for November 2007. However, no months after November 2007 were used; for example, the reference period for December 2008 included: December 2001, December 2002, December 2003, December 2004, December 2005, December 2006. This specific selection is essential to maintain uniformity among the reference periods considering Sidr made landfall in early November 2007. Anomalies were calculated until 2010 due to another cyclone that made landfall in Bangladesh in 2011. We did not want this to complicate our analysis which was focused solely on Sidr. An anomaly is calculated for the selected month of a year (January 2006–December 2010) by taking the difference between the chosen month and reference period means, then dividing by the standard deviation of the reference period [49]:

$$\text{NDVI anomaly} = \frac{\text{NDVI}_{\text{mean of a specific month}} - \text{NDVI}_{\text{mean of reference period}}}{\text{NDVI}_{\text{standard deviation of reference period}}} \tag{1}$$

Since the anomaly values are normalized by the reference period standard deviation, they are referred to as z-scores [49]. Upon classifying the z-scores at a later step, these values ultimately represent the severity of the event.

2.6. Reclassification and Summary Analysis

To facilitate area calculations, anomaly composites were summarized and reclassified into seasonal groups. The dry seasons included the months of November, December, and January. The mean of the seasonal composites was calculated and classified into four zones, High (z-scores < −5), Moderate (z-score > −5 and < −2.5), Low (z-score > −2.5 and < −1), and Neutral (z-score > −1 and < +1) (positive scores were classified using the same threshold). This classification indicates the severity of the damage (e.g., the lower the z-score the more severe damage sustained). Areas greater than +1 indicate positive anomalies, representing an increase in vegetation/photosynthetic activity compared to the reference period, and were omitted from further consideration. Areas that are between −1 to +1 are considered as neutral which indicates a vegetation condition within the long-term mean.

After the monthly MODIS anomaly z-scores were classified, they were categorized into different dry seasons based on the months included. The dry season represents the best window to obtain clear sky observations in this region of the world; therefore, multispectral image availability is substantially higher during the dry season in Bangladesh. Given our consideration of minimum satellite observations (we enforced four minimum observations per month), we believe these composites provide the most accurate assessment of satellite-derived vegetation productivity. Finally, the extent of the storm's impact was calculated by tabulating the area of classified severity zones based on the z-scores.

3. Results

3.1. Extent and Severity

The dry season anomaly of 2007 highlights the extent of the damage that occurred immediately after the cyclone (Figure 2A–C). South-eastern areas were most affected, south-western areas were moderately affected, and northern most areas least affected. This is consistent with the approximate path of Sidr (Figure 1C). The south-western and northern-most areas recovered more quickly than the south-eastern areas, as those areas were impacted more severely (Figure 2G). It is likely the November 2007 anomaly showed less damage than the December 2007 and January 2008 anomalies because November 2007 contains some pre storm pixels, as Sidr made landfall in the middle of November. The deviation in severity is more clear in the December 2007 and January 2008 anomalies compared to the November 2007 anomaly.

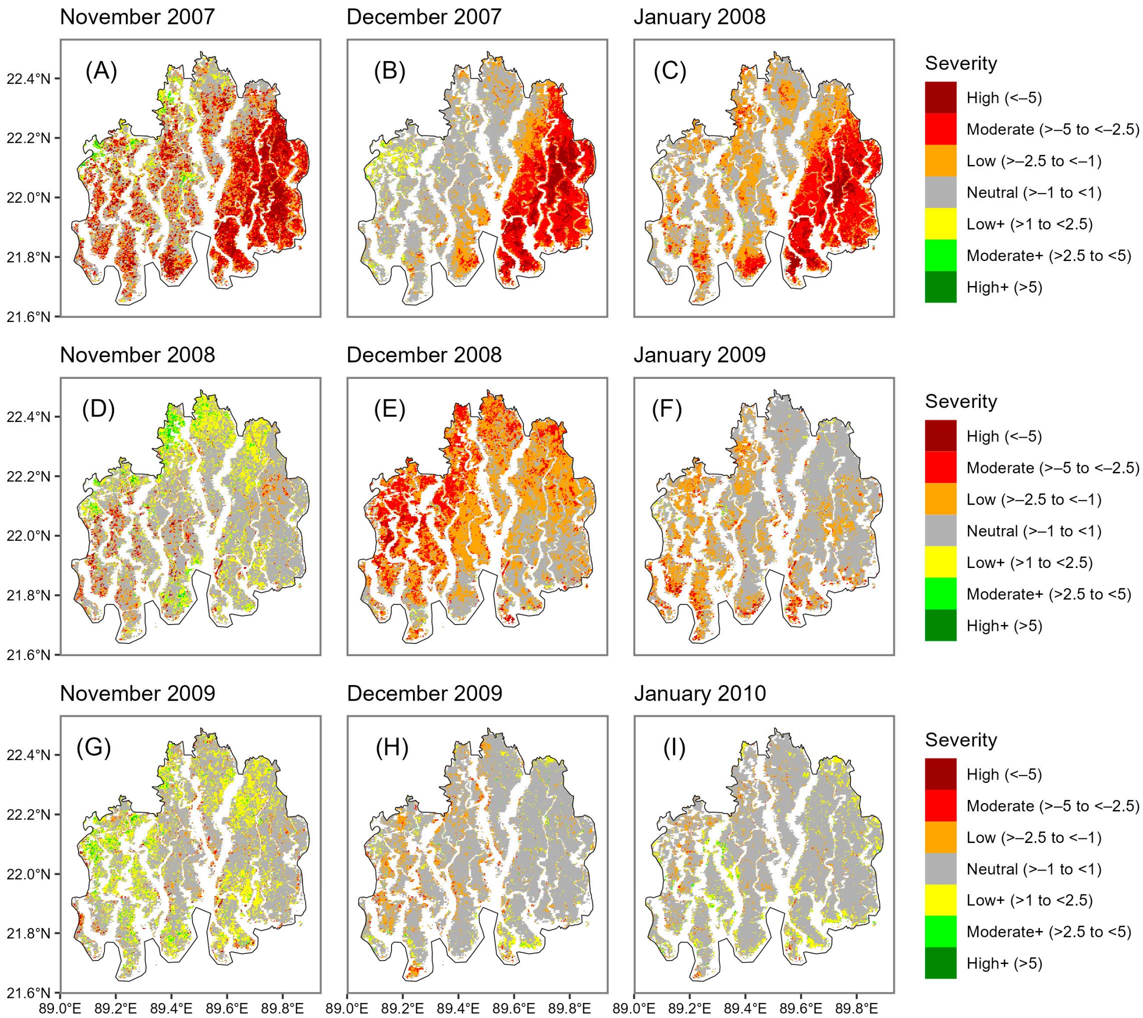

Figure 2. Monthly dry season anomalies: (**A**) November 2007, (**B**) December 2007, (**C**) January 2008, (**D**) November 2008, (**E**) December 2008, (**F**) January 2009, (**G**) November 2009, (**H**) December 2009, (**I**) January 2010. Negative anomalies represent damage compared to the reference period; whereas positive anomalies represent areas that performed higher than the reference period.

The dry season 2009 showed less variability in the high severity zone than the dry seasons of 2007 and 2008, indicating recovery of the areas heavily affected by Sidr (Figure 3). During this same time, neutral zones increased in area from dry season 2007 to 2009. The median z-score of neutral pixels was −0.32 in dry season 2007. However, it increased to 0.17 by the dry season 2009, although the high severity pixels increased at a slower rate. The median values of high severity pixels for dry season 2007 was −5.83 while the value remained similar (−5.98) in dry season 2009. However, moderate and low severity pixels showed improvement in median values over the dry seasons which adds consideration to the recovery question. The median of the moderate pixels decreased from −3.62 in dry season 2007 to −2.86 in dry season 2009 (Figure 3A–C). During that same period, the median of the low severity pixels also decreased from −1.6 to −1.28. These changes collectively indicate continuous post-Sidr recovery during that time period.

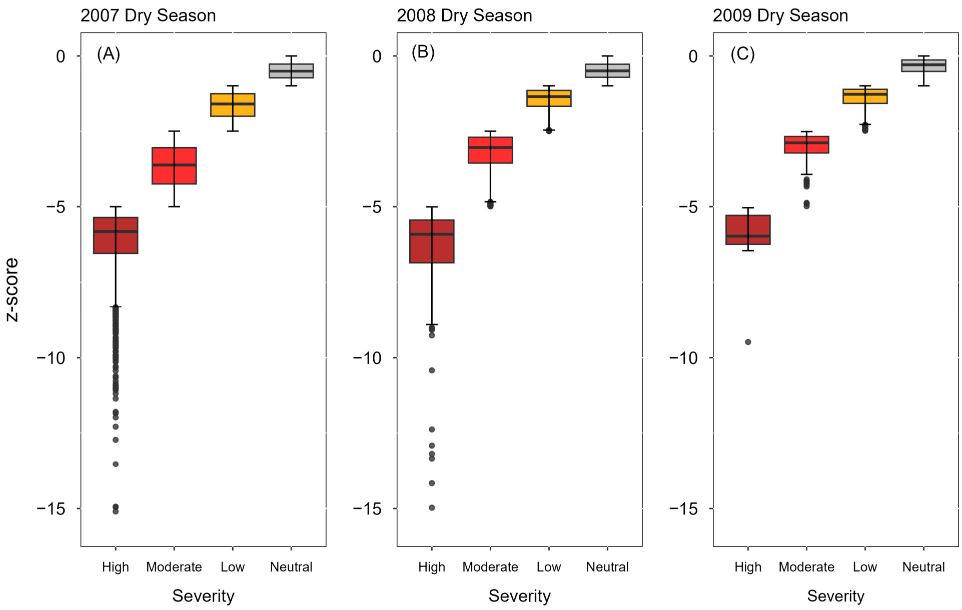

Figure 3. Dry season anomalies based on severity zones, (**A**) 2007 dry season, (**B**) 2008 dry season, and (**C**) 2009 dry season.

A total of approximately 2100 km^2 were impacted by cyclone Sidr during dry season 2007, which is 35% of the total Bangladesh Sundarbans area (approx. area 6000 km^2). The amount of damaged area was reduced to approximately 945 km^2 by dry season 2008 and 137 km^2 by dry season 2009 (Figure 4), a reduction in impacted area of 55% and 93% respectively. This decline indicates that damaged areas were slowly recovering from the cyclone's impact. An increase in the number of neutral areas (z-score > -1 to <+1) was also observed during the three consecutive dry seasons. There were 1460 km^2 of neutral pixels during dry season 2007. This increased to 2415 km^2 in dry season 2008 and 3040 km^2 in dry season 2009 (Figure 4C).

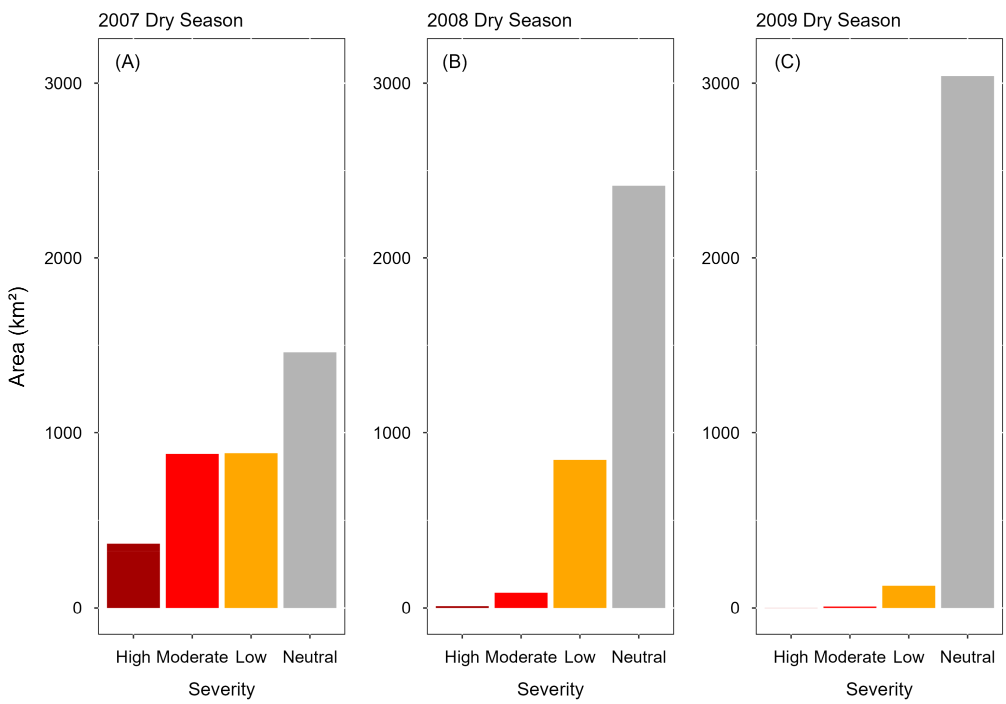

Figure 4. The extent of the post-Sidr damaged areas based on, (**A**) dry season 2007, (**B**) dry season 2008, (**C**) dry season 2009.

3.2. Post-Sidr Recovery

The recovery of z-scores, leading to a decrease in the size of high severity areas, coupled with an increase in area of with neutral z-scores, are all considered as recovery measures from Sidr. The number of high severity pixels decreased by 96% and 99% from dry season 2007 to dry season 2008 and 2009 consecutively (Figure 5). The mean area of high severity pixels was approximately 325 km^2 in dry season 2007, 11 km^2 in dry season 2008, and 750,000 m^2 (<1 km^2) in dry season 2009. A decline in the high severity pixels was also observed between the months in each season. This downward progression indicates slow recovery of highly impacted areas of the Sundarbans. Initially, the Sundarbans witnessed a severe loss in the eastern side of the Bangladesh side Sundarbans which recovered continuously with other severely affected areas in the whole Sundarbans (Figure 5).

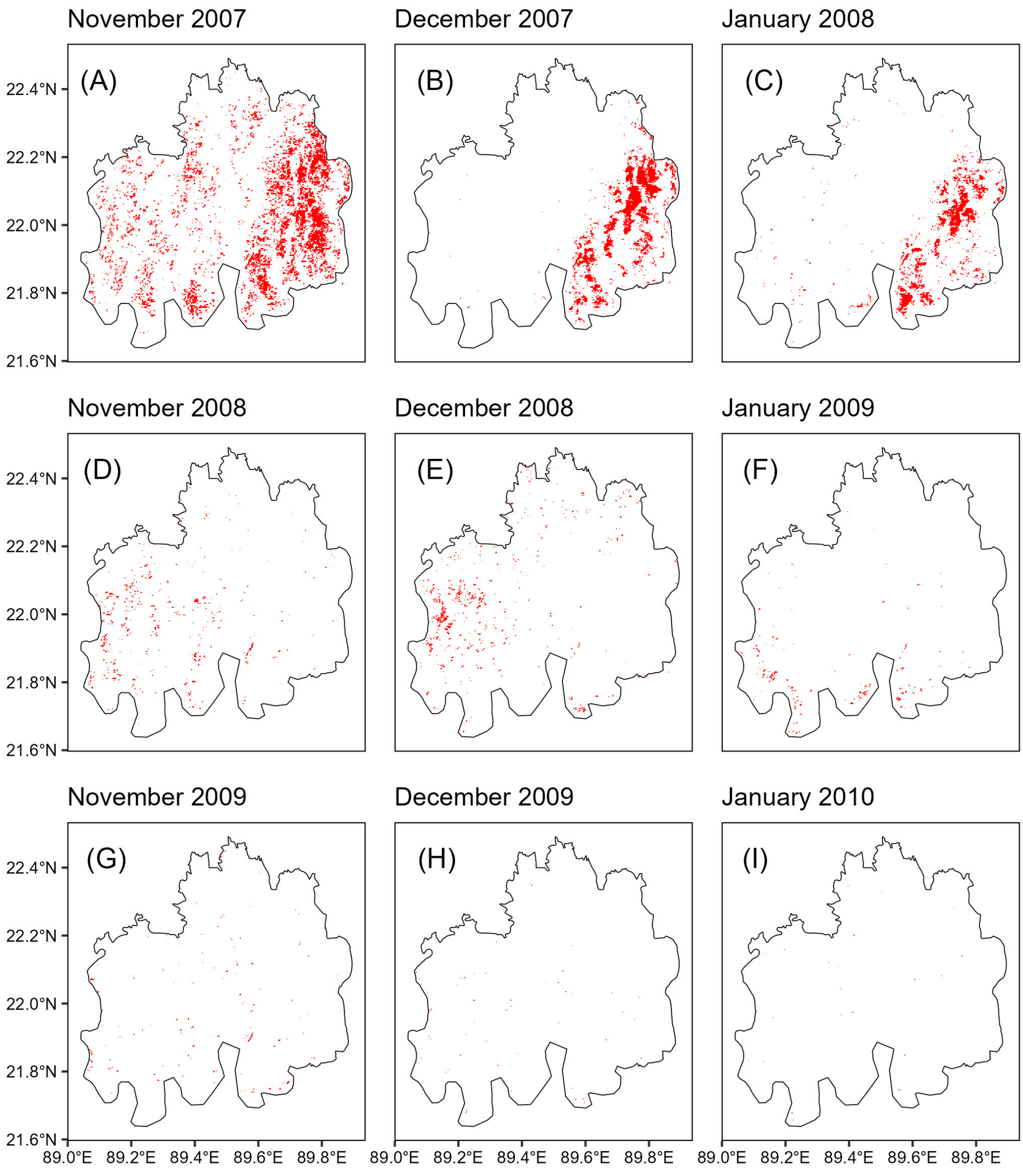

Figure 5. Recovery progression of areas that were impacted the greatest (high severity areas shown in red pixels) during the dry season: (**A**) November 2007, (**B**) December 2007, (**C**) January 2008, (**D**) November 2008, (**E**) December 2008, (**F**) January 2009, (**G**) November 2009, (**H**) December 2009, (**I**) January 2010.

In our review of the literature, we found little agreement between previous pixel-based studies of the impact of Sidr on the Sundarbans. Few studies attempted to assess the vegetation recovery from the event, and again, there was little agreement between findings (Table 1).

Table 1. Comparison of previous assessments on the extent of Sidr's impact. The delineation of severity and recovery period were included if assessed in the respective study.

Author	Sensor/Information Source	Approx. Affected Area (km^2)	High Severity Area (km^2)	Recovery Period
[51]	Expert opinion (based on site visit)	2400	NA	10–15 years
[52]	Expert opinion	1400	NA	30 years
[37]	ASTER	1330	149	NA
[36]	Landsat	2500	NA	3 years
[35]	MODIS	>8000 km^2 of the total Sundarbans has a disturbance severity of <10% [a]	NA	NA
[30]	SPOT-5	96 [b]	NA	NA
[38]	Landsat	726	NA	11 years (still ongoing at completion of study)
[32]	Landsat	1292	NA	NA
This study	MODIS	2090	325	2–3 years

[a] Highly impacted areas (eastern Sundarbans) identified spatially in their study area consistent with this study.
[b] Approximation based on the total study area (151 km^2) considered in the study.

4. Discussion

In this study, we considered disturbance as changes in forest structures due to cyclone which can cause high rate of tree mortality. We consider recovery as an increase in NDVI from a negative anomaly back to a neutral level. On the ground, this reflects a recovery of the photosynthetic capacity, through regrowth of leaves and branches. To explore the disturbance and recovery events, we employed a remote sensing approach to assess cyclone Sidr's impacts through a comparison of post-storm seasonal anomalies of vegetation condition compared to a reference period. Sidr impacted nearly 2100 km^2 (35% of the vegetated area) of the Bangladesh Sundarbans, with approximately 325 km^2 classified as high severity. Although we were unable to calculate a continuous monthly timeline due to extensive cloud cover in the region, the Sundarbans vegetation recovered substantially within three years from the event. After the third post-storm dry season (November 2009–January 2010), over 1950 km^2 (93% of the vegetated area) had recovered to the pre-storm reference period condition.

4.1. Extent and Severity of Cyclone Sidr

The most impacted landscape feature during a strong tropical cyclone is vegetation. Disturbances are a natural component of this ecosystem [53], but the high wind power of a tropical cyclone can cause extensive damage to vegetation. Sidr damaged 2090 km^2 of the total area of the Bangladesh Sundarbans during November 2007–January 2008; approximately 35% of vegetated areas. Our study identified severe vegetation damage in the vicinity of the cyclone trajectory on the south-eastern side of the Sundarbans (compare Figures 1 and 5), while the northern part was less affected. Vegetation outside of Sidr's direct path were likely damaged from the high winds associated with the storm event, with less damage at increasing distance from the storm's path (Figure 2).

These findings are spatially consistent with several other studies [36,37]. Akhter et al. [37] reported less damage to the vegetation (1330 km^2) however, this study only covered part of the Sundarbans and used imagery from a single day (21 November 2007) and was not able to capture delayed tree mortality from Sidr. The broader spatiotemporal resolution of our study enabled the long-term impact of delayed tree mortality across the entire Bangladesh Sundarbans to be assessed. Bhomik and Cabral [36] reported a similar amount of damage as our study (2500 km^2) and highlights the compatibility of different approaches and sensors

(Table 1). Although MODIS has reduced spatial resolution, it is consistent with Landsat based results [37], yet offers the additional temporal resolution for rapid assessment using monthly anomalies for immediate post-storm assessment. Awty-Carroll et al. [38] estimated the damage at just 726 km^2, however, they note their approach, using the Continuous Change Detection and Classification (CCDC) method was impacted by the Landsat 7 SLC error, which likely contributed to their lower damage estimate. They report most of the recovery occurred between 2013 and 2018, and 345 km^2 had not yet recovered by mid-2018, which is not consistent with our results or those of [36] (Table 1). There were 17 cyclones that made landfall in Bangladesh during their study period (1988–2018) [54], which could have impacted their results. Our results were consistent with a recent study using the MODIS Global Disturbance Index (MGDI), which uses Enhanced Vegetation Index (EVI) and Land Surface Temperature (LST) as inputs [35]. However, the MGDI did not appear to be as sensitive to vegetation damage as the EVI, likely due to moist soil reducing the impact on LST. Their EVI findings (50% decrease from pre-Sidr EVI in the eastern portion of the Sundarbans) spatially parallel to our NDVI results, which suggests that a vegetation index might outperform the MGDI in a mangrove ecosystem. Samanta et al. [55] observed deterioration in mangrove health in the Indian Sundarbans over the last 20 years using EVI and NDVI from Landsat and MODIS due to an increase in salinity and temperature, and decrease in pre- monsoon and post-monsoon rainfall. Such factors can influence post-cyclone mangrove recovery length.

The aforementioned studies did not consider a change based on a season, rather they focused on months or days. We focused on a season-based analysis, e.g., the primary months from dry-to-dry season, to depict the changes. Due to the tropical climate, it's not possible to obtain consistent clear sky images over the Sundarbans area, which may skew the results if not taken into consideration. Our results are mostly consistent with studies that used single date imagery at key points in time; however, the use of MODIS imagery in this study enabled season-based analysis with a robust reference period-based comparison and provides another line of evidence on the impact of Sidr.

The calculation of vegetation anomalies compares any study period (e.g., a month) with a known reference period, in a rapid, repeatable way [49]. In the context of climatic variability, a cyclone's impact on vegetation is a temporary condition, so anomalies are one of the most effective ways to explore the deviations from a given reference period [50]. Time series analysis is an effective method to show the trend in vegetation condition; however, we employed the anomaly analysis for two primary reasons. First, the analysis is rapid, highly repeatable, and easily interpreted. Second, it is more robust to the issue of missing observations than curve fitting. Missing observations in multispectral data are prevalent in this region given the extensive cloud cover during the wet season. Furthermore, we enforced a minimum observation threshold for a given composite period to minimize spurious values dependent on a single observation. Many studies do not account for this phenomenon, which could inaccurately portray the mean of a pixel over the time period of study.

4.2. Post-Sidr Recovery and Long-Term Vegetation Dynamics

Here, we report approximately 2100 km^2 (35% of the total area) of damage on the Bangladesh side of the Sundarbans. Over 1950 km^2 recovered by the dry season 2009 (November 2009, December 2009, and January 2010), a decline of 93%. The recovery is visible from November 2007 to January 2010 (compare Figures 2 and 3). Although we were unable to calculate a continuous monthly timeline due to extensive cloud cover, the Sundarbans vegetation recovered substantially within three years from the event.Bhomik and Cabral [36], using a Landsat and species-based approach, found the vegetation in the Sundarbans recovered by 2010 (Table 1). Conversely, Awty-Carroll et al. [38] reported approximately 345 km^2 of damaged pixels had not yet reached pre-Sidr level NDVI values by 2018. They noted a more rapid increase among the pixels between 2013 and 2018 than between 2007 and 2013 using their CCDC model. The authors note quick recovery of less exposed pixels and positive biasness of Landsat 8 NDVI, beginning in 2013, as reasons for this recovery difference, along with impacts from several other cyclones.

Divergent recovery estimates are possible as studies use different methods, spatial extents, time periods and imagery or expert opinion [51,52]. We found an approximate three-year recovery period, which is in agreement with [36] but differs from others (Table 1). Tropical cyclones can enhance mangrove forest growth by delivering nutrient-rich sediments [56] and soil accretion [57] which can aid in faster recovery. However, frequent cyclones can compound the recovery period of a single disaster event (e.g., Rashmi and Aila struck within three years of Sidr) (Table S1). Compound impacts of subsequent cyclones are often not considered in landscape scale studies [40,41]. Our results may also have been impacted by other unaccounted disturbances as evidenced by the spatial patterning of mapped high severity areas (compare Figure 5A–C with Figure 5D–F and Figure 5G–I). The east side of the Sundarbans has higher photosynthetic nitrogen use efficiency which could result in quicker recovery of damaged vegetation, whereas higher salinity on the west side might dampen recovery time [58]. Taken collectively, compound impacts likely reflect both a challenge and future need of landscape disturbance assessment in these systems. Estimates from remote sensing studies of mangrove recovery in other parts of the world vary from two to six years [31] to over a decade [17]. Numerous micro and macro factors govern recovery time and regional precipitation patterns are likely the primary difference at the global scale [14].

These issues, along with the range in the reported results of the extent and severity of Sidr, were a motivation for our analysis. Each approach offers strengths and weaknesses, however, our anomaly framework would allow analysts without advanced statistical training to detect vegetation change associated with cyclonic storm events could hold great value for rapid post-damage assessment. We acknowledge the coarse spatial resolution of MODIS data makes it more difficult to determine the precise rate of vegetation recovery due to spectral mixing of numerous ground elements. Therefore, this study provides another line of evidence about this historic ecosystem disturbance which could hold important clues about future disturbance impacts [59].

4.3. Limitations and Future Needs

In a MODIS pixel of approximately 250 × 250 m, many ecological processes are occurring at the same time and data misinterpretation is a possibility. For example, a low NDVI anomaly value might not represent decreased greenness of all the trees in a pixel; maybe only a portion is in decline. In the same way, a high NDVI anomaly value does not necessarily indicate the vegetation condition is uniformly higher across a given pixel. Some parts of it can be damaged but did not reflect in the main pixel analysis due to the coarse nature of the MODIS pixel. Furthermore, this issue could mask recovery processes at broad spatial scales and oversimplify ecological recovery processes. For example, high and moderate severity areas in the eastern portion of the study area in dry season 2007 appear to recover by dry season 2008 (compare Figure 2A–C with Figure 2D–F). Without timely field surveys, it is not possible to validate these results at this time given the retrospective view of this disturbance [59]. However, the temporal resolution of MODIS provides a robust series of observations for change detection analysis, particularly for areas like Sundarbans, where the inter-annual climate and cloud coverage is a huge obstacle for multispectral remote sensing. Fusion of medium-scale satellite imagery with fine-scale imagery collected by UAV holds great promise at local scales [17].

Climate change and anthropogenic factors are not addressed in this study since we focused on a single cyclonic event. Climate change influences tropical cyclone frequency and intensity [15]. Therefore, the relationship between climate change and mangrove forest recovery is a research need, as potential impacts are expected to increase in the future. This information would be a valuable contribution in better understanding the role of recovering mangrove forests in storm surge scenarios associated with future cyclone events [44]. Although the focus of our study was a single, cyclonic event, many anthropogenic disturbances are occurring in parts of the forest (e.g., fire, harvest, etc.) which is difficult information to obtain. However, future assessments should incorporate this information where possible to more accurately determine the recovery of cyclonic disturbances at local spatial scales. Recovery patterns and lag-effects likely differ by mangrove species and local environmental setting. A consideration of the influence of each of these aspects is a future research need, especially at local scales.

5. Conclusions

Remote sensing assessments provide key insights into the vegetation condition of an area after a severe disturbance. Furthermore, it is rarely possible to achieve such landscape scale insights in the absence of an extensive network of long-term ground monitoring data. Our results indicate Sidr impacted nearly 2100 km^2, 35% of the vegetated area in the Bangladesh Sundarbans. Given challenges with cloud-free observations during wet season months, we were unable to calculate a continuous timeline to evaluate vegetation recovery on a monthly time step. However, by the end of the third post-storm dry season (late January 2010) we documented 93% of the vegetated area had recovered to the pre-storm reference condition. Our results provide an additional line of evidence, consistent with some of the previous studies; however, it utilizes a methodology where it is possible to provide a rapid assessment of the vegetation damage shortly after the storm event. For example, our method can provide a comprehensive view of the extent of the damage, including lag effects on vegetation, in just a matter of months after the event. The ability to provide this information to natural resource managers in a timely fashion can be critical to select field monitoring locations and/or areas for restoration at local scales.

Supplementary Materials: The following supporting information can be downloaded at: https://www.mdpi.com/article/10.3390/coasts3030017/s1, Table S1. Recent cyclones that made landfall in Bay of Bengal (2007–2019) [42].

Author Contributions: Conceptualization, A.M.I. and T.J.A.; methodology, A.M.I. and T.J.A.; formal analysis, A.M.I.; data curation, A.M.I.; writing—original draft preparation, A.M.I. and T.J.A.; writing—review and editing, A.M.I. and T.J.A.; visualization, A.M.I.; supervision, T.J.A. All authors have read and agreed to the published version of the manuscript.

Funding: This research received no external funding.

Institutional Review Board Statement: Not applicable.

Informed Consent Statement: Not applicable.

Data Availability Statement: All satellite data used in this study are publicly available through Google Earth Engine. R code for analysis are available from the corresponding author upon request.

Acknowledgments: We thank Nicholas Manning for code development in Google Earth Engine. We gratefully acknowledge He Yin and Emariana Widner for reviewing an earlier version of this manuscript and the USGS Earth Resources Observation Systems Data Center for provision of satellite data.

Conflicts of Interest: The authors declare no conflict of interest.

References

1. Aziz, A.; Paul, A.R. Bangladesh Sundarbans: Present status of the Environment and Biota. *Diversity* **2015**, *7*, 242–269. [CrossRef]
2. Rahman, L.M. The Sundarbans: A Unique Wilderness of the World Legal Status. In *USDA Forest Service Proceedings RMRS-P-15-VOL-2*; U.S. Department of Agriculture, Forest Service, Rocky Mountain Research Station: Ogden, UT, USA, 2000; pp. 143–148. Available online: https://www.fs.usda.gov/research/treesearch/21939 (accessed on 1 January 2023).
3. Kanniah, K.D.; Sheikhi, A.; Cracknell, A.P.; Goh, H.C.; Tan, K.P.; Ho, C.S.; Rasli, F.N. Satellite images for monitoring mangrove cover changes in a fast growing economic region in southern Peninsular Malaysia. *Remote Sens.* **2015**, *7*, 14360–14385. [CrossRef]
4. Mazda, Y.; Magi, M.; Kogo, M. Phan Nguyen Hong Mangroves as a coastal protection from waves in the Tong King Delta, Vietnam. *Mangroves Salt Marshes* **1997**, *1*, 127–135. [CrossRef]
5. Kathiresan, K.; Rajendran, N. Coastal mangrove forests mitigated tsunami. *Estuar. Coast. Shelf Sci.* **2005**, *65*, 601–606. [CrossRef]

6. Das, S.; Vincent, J.R. Mangroves protected villages and reduced death toll during Indian super cyclone. *Proc. Natl. Acad. Sci. USA* **2009**, *106*, 7357–7360. [CrossRef]
7. Marois, D.E.; Mitsch, W.J. Coastal protection from tsunamis and cyclones provided by mangrove wetlands—A review. *Int. J. Biodivers. Sci. Ecosyst. Serv. Manag.* **2015**, *11*, 71–83. [CrossRef]
8. Sandilyan, S.; Kathiresan, K. Mangrove conservation: A global perspective. *Biodivers. Conserv.* **2012**, *21*, 3523–3542. [CrossRef]
9. Akber, M.A.; Patwary, M.M.; Islam, M.A.; Rahman, M.R. Storm protection service of the Sundarbans mangrove forest, Bangladesh. *Nat. Hazards* **2018**, *94*, 405–418. [CrossRef]
10. Karimi, Z.; Abdi, E.; Deljouei, A.; Cislaghi, A.; Shirvany, A.; Schwarz, M.; Hales, T.C. Vegetation-induced soil stabilization in coastal area: An example from a natural mangrove forest. *CATENA* **2022**, *216*, 106410. [CrossRef]
11. Sahoo, B.; Bhaskaran, P.K. Assessment on historical cyclone tracks in the Bay of Bengal, east coast of India. *Int. J. Climatol.* **2016**, *36*, 95–109. [CrossRef]
12. Ahmed, B.; Kelman, I.; Fehr, H.K.; Saha, M. Community resilience to cyclone disasters in coastal bangladesh. *Sustainability* **2016**, *8*, 805. [CrossRef]
13. Giri, C. Observation and monitoring of mangrove forests using remote sensing: Opportunities and challenges. *Remote Sens.* **2016**, *8*, 783. [CrossRef]
14. Pickett, S.T.A.; White, P.S. (Eds.) Natural Disturbance and Patch Dynamics: An Introduction. In *The Ecology of Natural Disturbance and Patch Dynamics*; Academic Press: Orlando, FL, USA, 1985; pp. 3–16.
15. Krauss, K.W.; Osland, M.J. Tropical cyclones and the organization of mangrove forests: A review. *Ann. Bot.* **2020**, *125*, 213–234. [CrossRef] [PubMed]
16. Sippo, J.Z.; Lovelock, C.E.; Santos, I.R.; Sanders, C.J.; Maher, D.T. Mangrove mortality in a changing climate: An overview. *Estuar. Coast. Shelf Sci.* **2018**, *215*, 241–249. [CrossRef]
17. Vizcaya-Martínez, D.A.; Flores-de-Santiago, F.; Valderrama-Landeros, L.; Serrano, D.; Rodríguez-Sobreyra, R.; Álvarez-Sánchez, L.F.; Flores-Verdugo, F. Monitoring detailed mangrove hurricane damage and early recovery using multisource remote sensing data. *J. Environ. Manag.* **2022**, *320*, 115830. [CrossRef]
18. Wang, W.; Qu, J.J.; Hao, X.; Liu, Y.; Stanturf, J.A. Post-hurricane forest damage assessment using satellite remote sensing. *Agric. For. Meteorol.* **2010**, *150*, 122–132. [CrossRef]
19. Sathish, C.; Nakhawa, A.D.; Bharti, V.S.; Jaiswar, A.K.; Deshmukhe, G. Estimation of extent of the mangrove defoliation caused by insect Hyblaea puera (Cramer, 1777) around Dharamtar creek, India using Sentinel 2 images. *Reg. Stud. Mar. Sci.* **2021**, *48*, 102054. [CrossRef]
20. Marra, D.M.; Chambers, J.Q.; Higuchi, N.; Trumbore, S.E.; Ribeiro, G.H.P.M.; dos Santos, J.; Negrón-Juárez, R.I.; Reu, B.; Wirth, C. Large-Scale Wind Disturbances Promote Tree Diversity in a Central Amazon Forest. *PLoS ONE* **2014**, *9*, e103711. [CrossRef]
21. Peereman, J.; Hogan, J.A.; Lin, T.-C. Assessing Typhoon-Induced Canopy Damage Using Vegetation Indices in the Fushan Experimental Forest, Taiwan. *Remote Sens.* **2020**, *12*, 1654. [CrossRef]
22. Cleland, E.; Chuine, I.; Menzel, A.; Mooney, H.; Schwartz, M. Shifting plant phenology in response to global change. *Trends Ecol. Evol.* **2007**, *22*, 357–365. [CrossRef]
23. Richardson, A.D.; Keenan, T.F.; Migliavacca, M.; Ryu, Y.; Sonnentag, O.; Toomey, M. Climate change, phenology, and phenological control of vegetation feedbacks to the climate system. *Agric. For. Meteorol.* **2013**, *169*, 156–173. [CrossRef]
24. Songsom, V.; Koedsin, W.; Ritchie, R.J.; Huete, A. Mangrove phenology and environmental drivers derived from remote sensing in Southern Thailand. *Remote Sens.* **2019**, *11*, 955. [CrossRef]
25. Valderrama-Landeros, L.; Flores-Verdugo, F.; Rodríguez-Sobreyra, R.; Kovacs, J.M.; Flores-de-Santiago, F. Extrapolating canopy phenology information using Sentinel-2 data and the Google Earth Engine platform to identify the optimal dates for remotely sensed image acquisition of semiarid mangroves. *J. Environ. Manag.* **2021**, *279*, 111617. [CrossRef] [PubMed]
26. Kamthonkiat, D.; Rodfai, C.; Saiwanrungkul, A.; Koshimura, S.; Matsuoka, M. Geoinformatics in mangrove monitoring: Damage and recovery after the 2004 Indian Ocean tsunami in Phang Nga, Thailand. *Nat. Hazards Earth Syst. Sci.* **2011**, *11*, 1851–1862. [CrossRef]
27. Macamo, C.C.F.; Massuanganhe, E.; Nicolau, D.K.; Bandeira, S.O.; Adams, J.B. Mangrove's response to cyclone Eline (2000): What is happening 14 years later. *Aquat. Bot.* **2016**, *134*, 10–17. [CrossRef]
28. Long, J.; Giri, C.; Primavera, J.; Trivedi, M. Damage and recovery assessment of the Philippines' mangroves following Super Typhoon Haiyan. *Mar. Pollut. Bull.* **2016**, *109*, 734–743. [CrossRef]
29. Zhang, K.; Thapa, B.; Ross, M.; Gann, D. Remote sensing of seasonal changes and disturbances in mangrove forest: A case study from South Florida. *Ecosphere* **2016**, *7*, e01366. [CrossRef]
30. Hoque, M.A.-A.; Phinn, S.; Roelfsema, C.; Childs, I. Assessing tropical cyclone impacts using object-based moderate spatial resolution image analysis: A case study in Bangladesh. *Int. J. Remote Sens.* **2016**, *37*, 5320–5343. [CrossRef]
31. Quader, M.A.; Agrawal, S.; Kervyn, M. Multi-decadal land cover evolution in the Sundarban, the largest mangrove forest in the world. *Ocean Coast. Manag.* **2017**, *139*, 113–124. [CrossRef]
32. Mandal, M.S.H.; Hosaka, T. Assessing cyclone disturbances (1988–2016) in the Sundarbans mangrove forests using Landsat and Google Earth Engine. *Nat. Hazards* **2020**, *102*, 133–150. [CrossRef]
33. Small, C.; Sousa, D. Spatiotemporal characterization of mangrove phenology and disturbance response: The Bangladesh Sundarban. *Remote Sens.* **2019**, *11*, 2063. [CrossRef]

34. Assal, T.J.; Anderson, P.J.; Sibold, J. Spatial and temporal trends of drought effects in a heterogeneous semi-arid forest ecosystem. *For. Ecol. Manag.* **2016**, *365*, 137–151. [CrossRef]
35. Dutta, D.; Das, P.K.; Paul, S.; Sharma, J.R.; Dadhwal, V.K. Assessment of ecological disturbance in the mangrove forest of Sundarbans caused by cyclones using MODIS time-series data (2001–2011). *Nat. Hazards* **2015**, *79*, 775–790. [CrossRef]
36. Bhowmik, A.; Cabral, P. *Damage and Post-Cyclone Regeneration Assessment of the Sundarbans Botanic Biodiversity Caused by the Cyclone Sidr*; The 1st World Sustainability Forum: Basel, Switzerland, 2011. [CrossRef]
37. Akhter, M.; Iqbal, Z.; Chowdhury, R.M. ASTER imagery of forest areas of Sundarban damaged by cyclone Sidr. *ISME/GLOMIS Electron. J.* **2008**, *6*, 5–7.
38. Awty-Carroll, K.; Bunting, P.; Hardy, A.; Bell, G. Using continuous change detection and classification of landsat data to investigate long-term mangrove dynamics in the Sundarbans region. *Remote Sens.* **2019**, *11*, 2833. [CrossRef]
39. Hoque, A.K.F.; Datta, D.K. The mangroves of Bangladesh. *Int. J. Ecol. Environ. Sci.* **2005**, *31*, 245–253.
40. Rahman, M.; Ullah, R.; Lan, M.; Sri Sumantyo, J.T.; Kuze, H.; Tateishi, R. Comparison of Landsat image classification methods for detecting mangrove forests in Sundarbans. *Int. J. Remote Sens.* **2013**, *34*, 1041–1056. [CrossRef]
41. Knapp, K.R.; Kruk, M.C.; Levinson, D.H.; Diamond, H.J.; Neumann, C.J. The International Best Track Archive for Climate Stewardship (IBTrACS): Unifying Tropical Cyclone Data. *Bull. Am. Meteorol. Soc.* **2010**, *91*, 363–376. [CrossRef]
42. IMD. Tracks of Cyclones and Depressions over North Indian Ocean (from 1891 onwards). 2011. Available online: https://rsmcnewdelhi.imd.gov.in/index.php (accessed on 26 May 2023).
43. Saffir, H. Hurricane Wind and Storm Surge. *Mil. Eng.* **1973**, *65*, 4.
44. Deb, M.; Ferreira, C.M. Potential impacts of the Sunderban mangrove degradation on future coastal flooding in Bangladesh. *J. Hydro-Environ. Res.* **2017**, *17*, 30–46. [CrossRef]
45. Cohen, W.B.; Healey, S.P.; Yang, Z.; Stehman, S.V.; Brewer, C.K.; Brooks, E.B.; Gorelick, N.; Huang, C.; Hughes, M.J.; Kennedy, R.E.; et al. How Similar Are Forest Disturbance Maps Derived from Different Landsat Time Series Algorithms? *Forests* **2017**, *8*, 98. [CrossRef]
46. Assal, T.J.; Steen, V.A.; Caltrider, T.; Cundy, T.; Stewart, C.; Manning, N.; Anderson, P.J. Monitoring long-term riparian vegetation trends to inform local habitat management in a mountainous environment. *Ecol. Indic.* **2021**, *127*, 107807. [CrossRef]
47. R Development Core Team. *R: A Language and Environment for Statistical Computing*; R Foundation for Statistical Computing: Vienna, Austria, 2013.
48. Hijmans, R.J.; van Etten, J. Raster: Geographic Data Analysis and Modeling. R package version 3.6-11. 2022. Available online: https://CRAN.R-project.org/package=raster (accessed on 5 September 2023).
49. Toomey, M.; Roberts, D.A.; Still, C.; Goulden, M.L.; McFadden, J.P. Remotely sensed heat anomalies linked with Amazonian forest biomass declines. *Geophys. Res. Lett.* **2011**, *38*, 1–5. [CrossRef]
50. Nanzad, L.; Zhang, J.; Tuvdendorj, B.; Nabil, M.; Zhang, S.; Bai, Y. NDVI anomaly for drought monitoring and its correlation with climate factors over Mongolia from 2000 to 2016. *J. Arid Environ.* **2019**, *164*, 69–77. [CrossRef]
51. UNESCO. Sundarbans World Heritage Site Devastated by Cyclone, According to UNESCO Experts Who Visited the Site. Available online: https://whc.unesco.org/en/news/399 (accessed on 5 March 2020).
52. Reliefweb. Bangladesh: Life-Saving Sundarbans May Take Years to Recover from Cyclone—Bangladesh. 2007. Available online: https://reliefweb.int/report/bangladesh/bangladesh-life-saving-sundarbans-may-take-years-recover-cyclone (accessed on 3 May 2020).
53. Hobbs, R.J.; Huenneke, L.F. Disturbance, Diversity, and Invasion: Implications for Conservation. *Conserv. Biol.* **1992**, *6*, 324–337. [CrossRef]
54. BMD. *List of Major Cyclonic Storms from 1960–2017*; Bangladesh Meteorological Department (BMD): Dhaka, Bangladesh, 2017. Available online: http://live.bmd.gov.bd/p/Historical-Cyclones/ (accessed on 7 October 2021).
55. Samanta, S.; Hazra, S.; Mondal, P.P.; Chanda, A.; Giri, S.; French, J.R.; Nicholls, R.J. Assessment and Attribution of Mangrove Forest Changes in the Indian Sundarbans from 2000 to 2020. *Remote Sens.* **2021**, *13*, 4957. [CrossRef]
56. Castañeda-Moya, E.; Rivera-Monroy, V.H.; Chambers, R.M.; Zhao, X.; Lamb-Wotton, L.; Gorsky, A.; Gaiser, E.E.; Troxler, T.G.; Kominoski, J.S.; Hiatt, M. Hurricanes fertilize mangrove forests in the Gulf of Mexico (Florida Everglades, USA). *Proc. Natl. Acad. Sci. USA* **2020**, *117*, 4831–4841. [CrossRef] [PubMed]
57. Rasquinha, D.N.; Mishra, D.R. Tropical cyclones shape mangrove productivity gradients in the Indian subcontinent. *Sci. Rep.* **2021**, *11*, 17355. [CrossRef]
58. Rahman, M.M.; Zhang, X.; Ahmed, I.; Iqbal, Z.; Zeraatpisheh, M.; Kanzaki, M.; Xu, M. Remote Sensing-Based Mapping of Senescent Leaf C:N Ratio in the Sundarbans Reserved Forest Using Machine Learning Techniques. *Remote Sens.* **2020**, *12*, 1375. [CrossRef]
59. Assal, T.J.; Sibold, J.; Reich, R. Modeling a Historical Mountain Pine Beetle Outbreak Using Landsat MSS and Multiple Lines of Evidence. *Remote Sens. Environ.* **2014**, *155*, 275–288. [CrossRef]